

# Pericyclic organometallic reactions. The reactions of $(\text{cht})\text{Fe}(\text{CO})_2\text{L}$ ( $\text{L} = \text{CO}, \text{P}(\text{OPh})_3, \text{PPh}_3$ ) and (carbomethoxy)maleic anhydride revisited<sup>☆</sup>

Zeev Goldschmidt\*, Elisheva Genizi, Hugo E. Gottlieb

Department of Chemistry, Bar-Ilan University, Ramat-Gan 52900, Israel

Received 21 April 1999; received in revised form 12 May 1999

Dedicated to Alberto Cecon to mark his 65th birthday

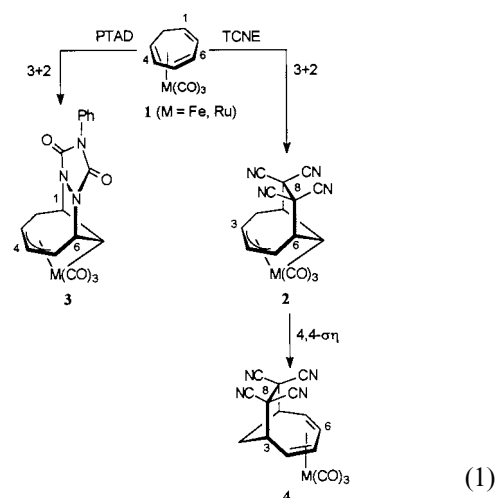
## Abstract

Kinetic studies of the reaction of  $(\text{cht})\text{Fe}(\text{CO})_2\text{L}$  ( $\text{L} = \text{CO}, \text{P}(\text{OPh})_3, \text{PPh}_3$ ) and (carbomethoxy)maleic anhydride reveal, contrary to our previous report, that the reactions proceed by a tandem 3 + 2-cycloaddition-[2,2]-sigmahaptotropic rearrangement, to give the corresponding  $\eta^2, \eta^2$ -Diels–Alder adducts as main products, in equilibrium with the primary  $\eta^1, \eta^3$ - $\sigma, \pi$ -allylic kinetic isomers. The labile primary isomers were characterized by <sup>1</sup>H-, <sup>13</sup>C- and <sup>31</sup>P-NMR spectra. Substitution of carbonyl by phosphorus ligands increased the rates of both cycloadditions and rearrangements in the order  $\text{PPh}_3 > \text{P}(\text{OPh})_3 > \text{CO}$ . © 1999 Elsevier Science S.A. All rights reserved.

**Keywords:** Cycloheptatriene; (Carbomethoxy)maleic anhydride; Iron complexes; Cycloadditions; Sigmahaptotropic rearrangements

## 1. Introduction

It has previously been shown that Group 8  $\text{M}(\text{CO})_3$  ( $\text{M} = \text{Fe}, \text{Ru}$ )  $\eta^4$ -complexes of cycloheptatriene (cht) **1** undergo selectively 3 + 2 cycloaddition reactions with highly electrophilic dienophiles such as tetracyanoethylene (TCNE) and 4-phenyl-1,2,4-triazoline-3,5-dione (PTAD), to give the corresponding 1,3- $\sigma, \pi$ -allylic complexes (**2** and **3**, respectively) as the primary kinetic products [1–4]. The iron adduct **2** ( $\text{M} = \text{Fe}$ ) further undergoes a thermal rearrangement to the formal 6 + 2 symmetrical  $\eta^4$ -adduct **4** via a pericyclic [4,4]-sigmahaptotropic ( $4,4-\sigma\eta$ ) shift [5,6], where the bridged  $\text{C}_8$  group  $\sigma$ -bonded to  $\text{C}_6$ , and the metal attached to  $\text{C}_3$ , exchange bonding sites antarafacially across the  $\pi$ -allylic chain (Eq. (1)). The corresponding ruthenium  $\sigma, \pi$ -allylic complexes **2**, **3** ( $\text{M} = \text{Ru}$ ) remain stable under similar thermal conditions [4].



Unexpectedly, the powerful dienophile (carbomethoxy)maleic anhydride (CMA) **5**, first reported by Hall et al. [7], appeared to depart from the general 3 + 2 cycloaddition rule. The reaction of CMA with  $(\text{cht})\text{Fe}(\text{CO})_3$  (**1**) ( $\text{M} = \text{Fe}$ ) solely afforded the formal Diels–Alder 4 + 2 adduct **6** (Eq. (2)) [8]. Since both 3 + 2 and 4 + 2 cycloadditions are thermally allowed pericyclic reactions [8,3], we contemplated that the cyclic anhydride group is responsible for the switch in

<sup>☆</sup> Previous paper in this series: Ref. [4].

\* Corresponding author. Fax: +972-3-5351250.

E-mail address: goldz@mail.biu.ac.il (Z. Goldschmidt)

the reaction periselectively [8]. However, we later found that CMA reacts with the isolobal  $(\text{cht})\text{Ru}(\text{CO})_3$  (**1**) ( $M = \text{Ru}$ ) complex in the usual 3 + 2 manner, affording the stable  $\sigma, \pi$ -allylic adduct **7** [4]. This led us to re-examine our previous conclusions by looking more carefully at the initial stages of this reaction. Here, we wish to present the details of a kinetic study of the reaction of  $(\text{cht})\text{Fe}(\text{CO})_3$  (**1**) and CMA, with extension to the phosphorus containing analogous complexes  $(\text{cht})\text{Fe}(\text{CO})_2\text{L}$  (**1**) ( $L = \text{P}(\text{OPh})_3, \text{PPh}_3$ ) [9–11].

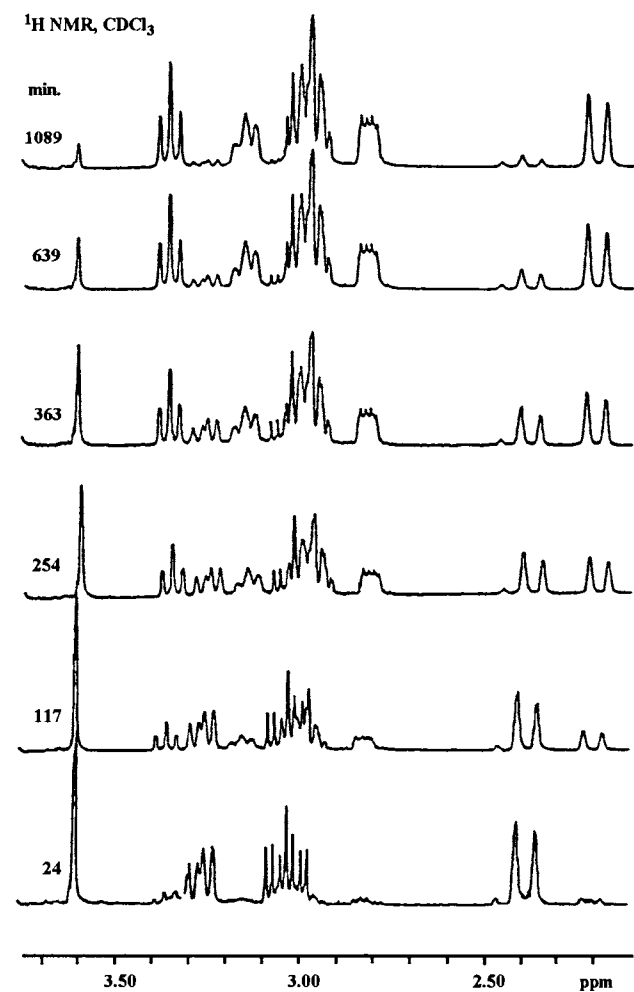
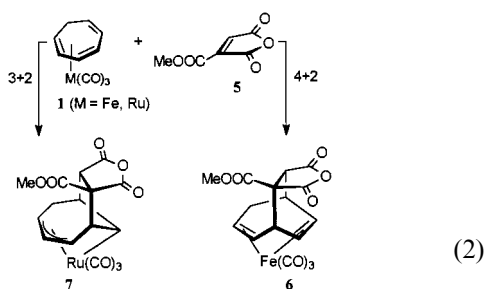
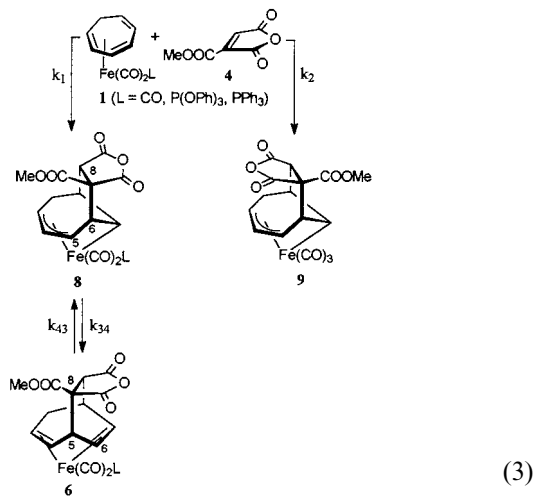


Fig. 1. Time resolved  $^1\text{H}$ -NMR spectra of the [2,2]-sigmahaptotropic rearrangement of **8**  $\rightarrow$  **6**.

## 2. Results

A 1:1 molar ratio of **1** and CMA was directly dissolved in  $\text{CDCl}_3$  in an NMR tube in order to allow immediate recording of the spectrum. The reaction progress was followed from the time-resolved  $^1\text{H}$ -NMR spectra, shown in Fig. 1. The spectra reveal the primary formation of a major kinetic product, whose structural assignment as the  $\sigma, \pi$ -allylic complex **8** is based on the characteristic high field  $^1\text{H}$ -NMR signal at  $\delta$  1.25, and the close resemblance to the related  $\sigma, \pi$ -allylic adduct of **1** ( $M = \text{Fe}$ ) and TCNE [6] (Tables 1 and 2). The formation of another primary adduct, whose concentration in the reaction mixture quickly reached a maximum of 5%, was also detected. The NMR signals of this minor product appear as satellites of **8**, hence, we assigned its structure as the *endo*-anhydride regioisomer **9**. None of these primary adducts could be isolated.

While the concentration of the minor adduct **9** remains constant after ca. 20 min, **8** is labile under the reaction conditions and readily undergoes rearrangement to form the 4 + 2 isomer **6**, which was previously isolated and whose structure was confirmed by single-crystal X-ray analysis [8]. An equilibrium mixture is reached with a 24:1 ratio of **6**:**8**. The overall reaction of **1** with CMA is thus summarized in Eq. (3).



Analysis of the rearrangement reveals the antarafacial migratory exchange of the bridged  $\text{C}_8$  malonate moiety with the metal bonded to  $\text{C}_5$  across the  $\text{C}_5$ – $\text{C}_6$  bond. This corresponds to a new member of the [2,2]-sigmahaptotropic ( $2,2$ - $\sigma, \eta$ ) rearrangements, between a  $\eta^1, \eta^3$ - $\sigma, \pi$ -allylic complex and a  $\eta^2, \eta^2$ -di- $\pi$ -methane complex. A related  $2,2$ - $\sigma, \eta$  rearrangement of an allylic  $\sigma$ -bond in a  $\eta^4$ -diene complex to a  $\eta^1, \eta^3$ - $\sigma, \pi$ -allylic complex, shown in Eq. (4), has been previously reported by us [12].

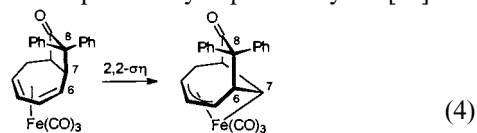


Table 1  
<sup>1</sup>H-NMR spectra of (cht)Fe(CO)<sub>2</sub>L adducts with CMA<sup>a</sup>

	H <sub>1</sub>	H <sub>2s</sub>	H <sub>2a</sub>	H <sub>3</sub>	H <sub>4</sub>	H <sub>5</sub>	H <sub>6</sub>	H <sub>7</sub>	H <sub>9</sub>
<b>8</b> (L = CO)	3.27	3.04	2.40	4.57	4.34	4.65	3.93	1.25	3.60
3.92 (CO <sub>2</sub> Me)	<i>J</i> <sub>1,2s</sub> = 11.5; <i>J</i> <sub>1,2a</sub> = 1.5; <i>J</i> <sub>1,3</sub> = <i>J</i> <sub>1,6</sub> = 0.5; <i>J</i> <sub>1,7</sub> = 7.5; <i>J</i> <sub>1,9</sub> = 0.7; <i>J</i> <sub>2s,2a</sub> = 17.0; <i>J</i> <sub>2s,3</sub> = 5.5; <i>J</i> <sub>2a,3</sub> = <i>J</i> <sub>2a,4</sub> = 1.5; <i>J</i> <sub>3,4</sub> = 9.2; <i>J</i> <sub>3,5</sub> = 0.8; <i>J</i> <sub>4,5</sub> = 7.2; <i>J</i> <sub>4,6</sub> = 0.5; <i>J</i> <sub>5,6</sub> = 7.0; <i>J</i> <sub>5,7</sub> = 1.5; <i>J</i> <sub>6,7</sub> = 9.0								
<b>9</b> <sup>b</sup>	3.27	3.0	2.4	4.5	4.4	4.73	3.9	1.5	3.60
3.92 (CO <sub>2</sub> Me)	<i>J</i> <sub>1,2s</sub> = 12; <i>J</i> <sub>1,7</sub> = 8; <i>J</i> <sub>2s,2a</sub> = 17; <i>J</i> <sub>2s,3</sub> = 5; <i>J</i> <sub>3,4</sub> ≈ 10; <i>J</i> <sub>4,5</sub> ≈ <i>J</i> <sub>5,6</sub> ≈ 7.5; <i>J</i> <sub>5,7</sub> = 1.6								
<b>8</b> (L = P(OPh) <sub>3</sub> ) <sup>c</sup>	+ 3.21	2.90	2.19	4.08	4.25	3.18	3.73	1.02	3.57
3.84 (CO <sub>2</sub> Me), 7.15–7.40 (Ph)	<i>J</i> <sub>1,2s</sub> = 12; <i>J</i> <sub>1,7</sub> = 7; <i>J</i> <sub>2s,2a</sub> = 16; <i>J</i> <sub>2s,3</sub> = 5; <i>J</i> <sub>3,4</sub> = <i>J</i> <sub>4,5</sub> = 8; <i>J</i> <sub>5,6</sub> = 7; <i>J</i> <sub>6,7</sub> = 9; <i>J</i> <sub>4P</sub> = 8								
<b>6</b> (L = CO)	3.16	3.00	2.21	2.84	3.36	4.28	3.01	2.96	3.79
3.90 (CO <sub>2</sub> Me)	<i>J</i> <sub>1,2s</sub> = <i>J</i> <sub>1,7</sub> = 8.0; <i>J</i> <sub>1,8</sub> = 2.5; <i>J</i> <sub>2s,2a</sub> = 16.0; <i>J</i> <sub>2s,3</sub> = 6.5; <i>J</i> <sub>2a,3</sub> = 1.5; <i>J</i> <sub>2a,4</sub> = 1.0; <i>J</i> <sub>3,4</sub> = 8.0; <i>J</i> <sub>3,5</sub> ≈ 0.5; <i>J</i> <sub>4,5</sub> = 8.0; <i>J</i> <sub>5,6</sub> = 4.0; <i>J</i> <sub>5,7</sub> = 1.5; <i>J</i> <sub>6,7</sub> = 8.0								
<b>6</b> (L = P(OPh) <sub>3</sub> )	2.97	2.93	2.05	2.35	2.82	3.34	2.31	2.57	3.64
3.83 (CO <sub>2</sub> Me), 7.18–7.41 (Ph)	<i>J</i> <sub>1,2s</sub> = 9.5; <i>J</i> <sub>1,7</sub> = 7.0; <i>J</i> <sub>1,8</sub> = 2.5; <i>J</i> <sub>2s,2a</sub> = 15.0; <i>J</i> <sub>2s,3</sub> = 4.0; <i>J</i> <sub>2a,4</sub> ≈ 0.5; <i>J</i> <sub>3,4</sub> = 8.5; <i>J</i> <sub>4,5</sub> = 8.0; <i>J</i> <sub>5,6</sub> = 7.0; <i>J</i> <sub>5,7</sub> = 1.5; <i>J</i> <sub>6,7</sub> = 7.0; <i>J</i> <sub>7,8</sub> ≈ 0.5; <i>J</i> <sub>4,P</sub> = 6.0; <i>J</i> <sub>6,P</sub> = 7.0								
<sup>d</sup> 3.00	3.00	2.23	2.46	3.00	3.35	2.51	2.65	3.84	
<b>6</b> (L = PPh <sub>3</sub> )	2.95	3.16	2.23	2.61	3.01	4.37	1.91	1.69	3.64
3.89 (CO <sub>2</sub> Me), 7.30–7.60 (Ph)	<i>J</i> <sub>1,2s</sub> = 9.5; <i>J</i> <sub>1,7</sub> = 8.0; <i>J</i> <sub>1,8</sub> = 2.5; <i>J</i> <sub>1,2a</sub> = 2.0; <i>J</i> <sub>1,3</sub> ≈ 1.0; <i>J</i> <sub>1,6</sub> ≈ 0.5; <i>J</i> <sub>2s,2a</sub> = 15.0; <i>J</i> <sub>2s,3</sub> = 4.0; <i>J</i> <sub>2a,4</sub> = <i>J</i> <sub>2s,4</sub> ≈ 0.5; <i>J</i> <sub>3,4</sub> = 8.5; <i>J</i> <sub>4,5</sub> = 8.0; <i>J</i> <sub>5,6</sub> = 7.0; <i>J</i> <sub>5,7</sub> = 1.5; <i>J</i> <sub>6,7</sub> = 6.5; <i>J</i> <sub>6,P</sub> = 9.5; <i>J</i> <sub>7,P</sub> = 2.0								

<sup>a</sup> 300 MHz,  $\delta$  in ppm from TMS, *J* in Hz, *s*, *syn*; *a*, *anti* to the metal.

<sup>b</sup> Low concentrations and overlap of peaks with **8** prevented accurate signal assignment.

<sup>c</sup> This isomer was observed only at low temperatures.

<sup>d</sup> In acetone-*d*<sub>6</sub>.

When (cht)Fe(CO)<sub>2</sub>P(OPh)<sub>3</sub> and (cht)Fe(CO)<sub>2</sub>PPh<sub>3</sub> react with CMA, a similar two-step reaction pattern was observed. However, only the 3 + 2 *exo*-regioisomers **8** (L = P(OPh)<sub>3</sub>, PPh<sub>3</sub>) were detected in the cycloaddition step, and the rearrangements to **6** (L = P(OPh)<sub>3</sub>, PPh<sub>3</sub>) proceed practically to completion (*k*<sub>34</sub> ≫ *k*<sub>43</sub>). Both cycloadditions and rearrangements are faster than those of the parent tricarbonyl derivative in the order PPh<sub>3</sub> > P(OPh)<sub>3</sub> > CO. The enhancement due to phosphorus ligands is a general phenomenon in iron carbonyl complexes, and has been observed e.g. in the related reaction of (tropone)Fe(CO)<sub>2</sub>PPh<sub>3</sub> with TCNE [13], and in the rotational barriers of η<sup>4</sup>-butadiene complexes [14].

### 3. Kinetic studies

In order to simplify the kinetic calculations we used equimolar amounts of the reactants **1** and CMA in all

experiments. The initial concentrations of the reactants *C*<sub>0</sub> = 50 mM. Reactions were carried out in CDCl<sub>3</sub> solutions at 24°C, and followed by <sup>1</sup>H-NMR (Fig. 1). The relative concentrations of **1** and the reaction products were derived by integration of the relevant proton signals.

The initial rate constant *k*<sub>obs</sub> for the cycloaddition reaction was determined from the second-order rate Eq. (5), from the slope of the plot of 1/[**1**] versus time (*t*) [15,16]. This rate constant *k*<sub>obs</sub> = *k*<sub>1</sub> + *k*<sub>2</sub>, where *k*<sub>1</sub> and *k*<sub>2</sub> are the rate constants of the formation of **8** and **9**, respectively (Eq. (3)). Since **9** remains constant during the rearrangement, the ratio between the cycloaddition rate constants can be determined from Eq. (6), and consequently both *k*<sub>1</sub> and *k*<sub>2</sub> can be estimated from Eqs. (5) and (6). The initial first-order rate constant of the rearrangement of **8** to **6** *k*<sub>34</sub> was similarly estimated (Eq. (7)) from the slope of the line obtained by plotting ln [**8**] versus time, for values taken after completion of the cycloaddition step (ca. 40 min).

Table 2  
 $^{13}\text{C}$ -NMR spectra of adducts of (cht)Fe(CO) $_2$ L complexes with CMA <sup>a</sup>

	C <sub>1</sub>	C <sub>2</sub>	C <sub>3</sub>	C <sub>4</sub>	C <sub>5</sub>	C <sub>6</sub>	C <sub>7</sub>
<b>8</b> (L = CO)	57.3	40.4	76.7	97.0	62.5	58.1	20.9
58.1 (C <sub>8</sub> ), 63.3 (C <sub>9</sub> ), 53.1 (Me), 212.8, 211.0, 202.4 (ligand CO), 171.3 (ester), 167.9, 164.9 (anhydride)							
<b>6</b> (L = CO)	33.8	40.8	71.6	45.5	37.9	24.1	59.8
51.2 (C <sub>8</sub> ), 63.3 (C <sub>9</sub> ), 54.1 (Me, $J_{\text{C,H}} = 149$ ), 214.0 (ligand CO), 170.0 (ester), 167.5, 166.0 (anhydride)							
$J_{\text{C,H}}$	140	131	160	173	150	176	165
<b>6<sup>b</sup></b> (L = P(OPh) <sub>3</sub> )	35.0	41.5	71.0	42.2	39.5	23.8	60.3
51.7 (C <sub>8</sub> ), 64.1 (C <sub>9</sub> ), 53.7 (Me), 219.7 ( $J_{\text{C,P}} = 25$ ), 219.4 ( $J_{\text{C,P}} = 21$ ) (ligand CO), 171.7 (ester), 168.6, 166.7 (anhydride), 152.3 (C <sub>ipso</sub> , $J_{\text{C,P}} = 7$ ), 130.6 (C <sub>meta</sub> ) 126.1 (C <sub>para</sub> ) 122.2 (C <sub>ortho</sub> , $J_{\text{C,P}} = 4$ )							
$J_{\text{C,P}}$	–	3	2	–	–	4	6

<sup>a</sup> 300 MHz,  $\delta$  in ppm from TMS,  $J$  in Hz.

<sup>b</sup> In acetone- $d_6$ .

$$1/[1]_t - 1/[1]_0 = k_{\text{obs}}t = (k_1 + k_2)t \quad (5)$$

$$k_1/k_2 = ([8] + [6])/[9] \quad (6)$$

$$\ln [8] = k_{34}t \quad (7)$$

The rate constants thus obtained were used as the initial values for the set of the four equations (Eqs. (8)–(11)) in a numeric simulation program which describes the overall pathway of the reaction, as outlined in Eq. (3).

$$d[1]/dt = -(k_1 + k_2)[1]^2 \quad (8)$$

$$d[8]/dt = k_1[1]^2 - k_{34}[8] + k_{43}[6] \quad (9)$$

$$d[9]/dt = k_2[1]^2 \quad (10)$$

$$d[6]/dt = k_{34}[8] - k_{43}[6] \quad (11)$$

The specific values of the rate constants were derived by modification of the initial values until a best fit to the experimental points was obtained. Since the cycloaddition reaction to **8** is much faster than the following rearrangement to **6**, the fitting results for the cycloaddition part is illustrated in Fig. 2, whereas those for the rearrangement are depicted in Fig. 3.

The same experiment was repeated at a higher temperature of 43°C in order to evaluate the activation parameters of the cycloadditions and the rearrangement. Cycloaddition was too fast to be measured accurately. The experimental data for the rearrangement were collected over 2 h, whereby the rearrangement proceeded to the extent of over 90%. The results were evaluated by the simulation program as above. The overall reaction progress is depicted in Fig. 4. The kinetic data are collected in Table 3.

The reactions of the phosphorus complexes **1** (L = P(OPh)<sub>3</sub>, PPh<sub>3</sub>) with CMA were followed by  $^{31}\text{P}$ -NMR. When the reactions were conducted at ambient temper-

ature only the rearranged products **6** were essentially observed. Hence, low temperature experiments were carried out in CDCl<sub>3</sub> with a 1:1 ratio of **1** (L = P(OPh)<sub>3</sub>) and **5**, at –33 and –17°C, following the signals at 162.7 and 172.3 ppm of **8** and **6** (L = P(OPh)<sub>3</sub>), respectively. The rearrangement in acetone- $d_6$  is surprisingly slower than in chloroform but is accompanied by extensive polymerization of CMA [17] to phosphorus-containing polymer(s) (by NMR). This required the addition of excess of CMA in order to consume the complex. However, the use of excess of

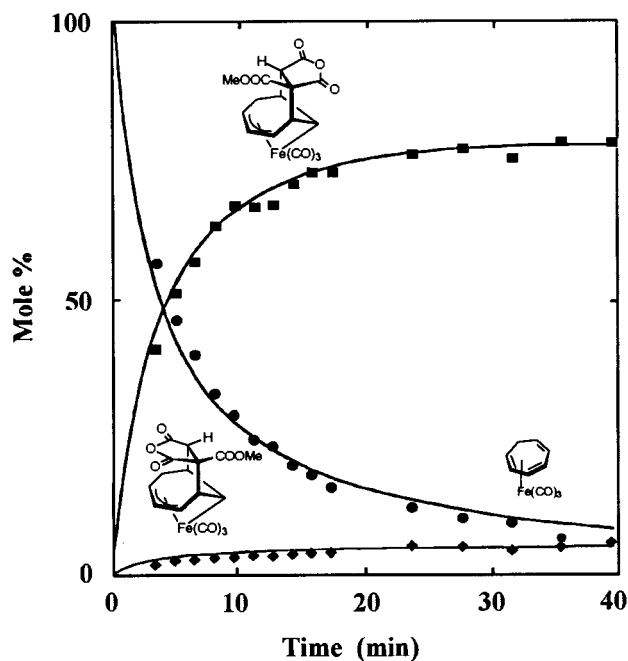


Fig. 2. Progress of the cycloaddition of (cht)Fe(CO)<sub>3</sub> and (carbomethoxy)maleic anhydride.

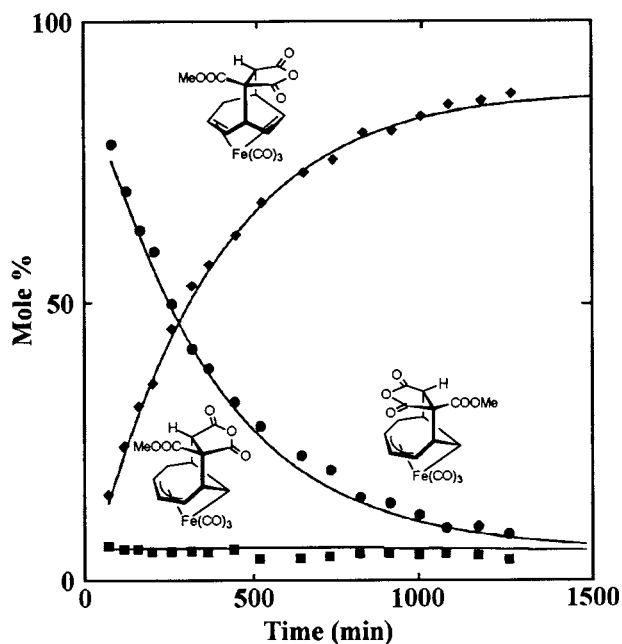


Fig. 3. Progress of the [2,2]-sigmahaptotropic rearrangement of **8** to **6**.

either of the reactants did not considerably effect the rearrangement rates, regardless of the presence of the polymer. Experiments were thus conducted using four-fold excess CMA, at 12 and 25°C, and monitored as above by integration of the respective phosphorus sig-

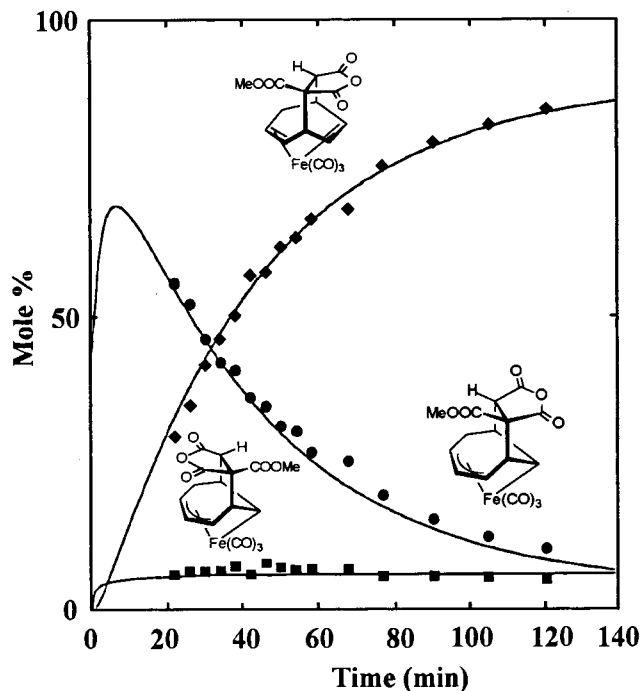


Fig. 4. Progress of the tandem reaction of  $(\text{cht})\text{Fe}(\text{CO})_3$  and (carboxymethoxy)maleic anhydride (the disappearance of the starting complex is not shown for clarity. See Fig. 2 however).

Table 3

Kinetic data of the reactions of  $(\text{cht})\text{Fe}(\text{CO})_2\text{L}$  with CMA <sup>a</sup>

	$k_1$ ( $\text{M}^{-1} \text{s}^{-1}$ )	$k_2$ ( $\text{M}^{-1} \text{s}^{-1}$ )	$k_{34}$ ( $\text{s}^{-1}$ )	$k_{43}$ ( $\text{s}^{-1}$ )
<b>I</b> ( $L = \text{CO}$ )				
298 K	$8.28 \times 10^{-2}$	$5.26 \times 10^{-3}$	$4.58 \times 10^{-5}$	$2.92 \times 10^{-6}$
318 K	$2.17 \times 10^{-1}$	$1.12 \times 10^{-2}$	$4.08 \times 10^{-4}$	$1.58 \times 10^{-5}$
$\Delta G^\ddagger$ (kcal mol <sup>-1</sup> )				
298 K	18.92	18.35	23.36	24.99
318 K	21.97	21.49	23.59	25.64
<b>1</b> → <b>8</b>	$\Delta H^\ddagger = 8.5$ kcal mol <sup>-1</sup>		$\Delta S^\ddagger = -35$ e.u.	
<b>8</b> → <b>6</b>	$\Delta H^\ddagger = 20.0$ kcal mol <sup>-1</sup>		$\Delta S^\ddagger = -11$ e.u.	
<b>I</b> ( $L = P(\text{O}Ph)_3$ )				
256 K			$4.15 \times 10^{-4}$	
240 K			$6.03 \times 10^{-5}$	
<b>8</b> → <b>6</b>	$\Delta G_{256}^\ddagger = 18.9$ kcal mol <sup>-1</sup>			
	$\Delta G_{240}^\ddagger = 18.6$ kcal mol <sup>-1</sup>			
	$\Delta H^\ddagger = 14.3$ kcal mol <sup>-1</sup>		$\Delta S^\ddagger = -18$ e.u.	
298 K <sup>b</sup>			$4.80 \times 10^{-5}$	
285 K <sup>b</sup>			$4.65 \times 10^{-6}$	
<b>8</b> → <b>6</b>	$\Delta G_{298}^\ddagger = 23.3$ kcal mol <sup>-1</sup>			
	$\Delta G_{285}^\ddagger = 23.61$ kcal mol <sup>-1</sup>			
	$\Delta H^\ddagger = 29.5$ kcal mol <sup>-1</sup>		$\Delta S^\ddagger = 21$ e.u.	
<b>I</b> ( $L = PPh_3$ )				
<b>8</b> → <b>6</b>			$1.79 \times 10^{-4}$	$1.4 \times 10^{-5}$
234 K			17.60	18.78
$\Delta G^\ddagger$ (kcal mol <sup>-1</sup> )				

<sup>a</sup> Reactions performed in  $\text{CDCl}_3$ .

<sup>b</sup> In  $(\text{CD}_3)_2\text{CO}$ .

nals. The first-order constants of the rearrangement were derived from the slopes of  $\ln(\%8)$  versus time (Fig. 5). The kinetic data are collected in Table 3.

In order to follow the rearrangement of **8** to **6** ( $L = PPh_3$ ), the reaction of **1** with CMA was conducted in  $\text{CDCl}_3$  at  $-39^\circ\text{C}$ . The equilibrium constant  $6/8 = K_{\text{eq}} = 0.078$  was determined from the <sup>31</sup>P-NMR spec-

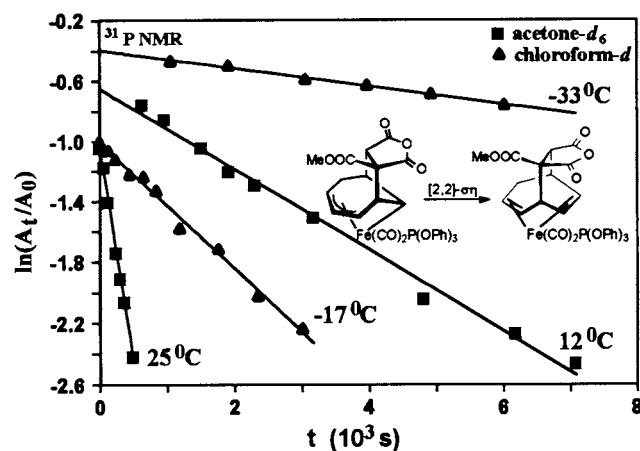


Fig. 5. Progress of the [2,2]-sigmahaptotropic rearrangement of phosphorus **8** in acetone chloroform.

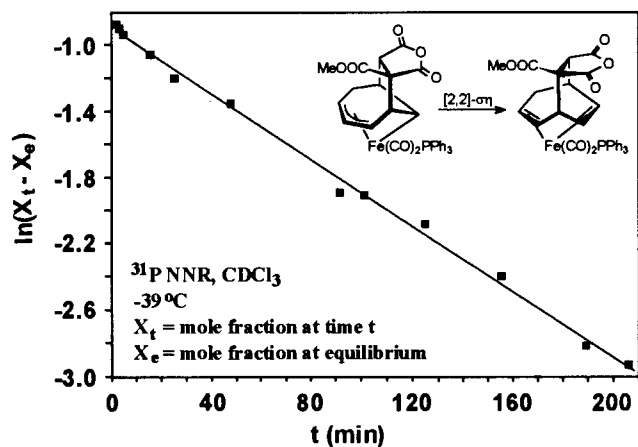


Fig. 6. Progress of the [2,2]-sigmahaptotropic rearrangement of phosphite **8**.

trum ( $\delta = 58.6$  and  $81.0$  ppm, respectively) by extrapolation of the ratio between the isomers. The kinetic constants were determined from the slope of  $\ln(X_t - X_e)$  versus time, where  $X_t$  and  $X_e$  are the mole fractions of **8** at time  $t$  and at equilibrium, respectively (Fig. 6).

#### 4. Conclusions

Our present studies of the reaction of CMA with the (cht)Fe(CO)<sub>3</sub> complex show that the 4 + 2 Diels–Alder adduct **6**, previously reported [8] as being the one step kinetic product of the reaction, is in fact the thermodynamic product of a fast tandem 3 + 2 cycloaddition–[2,2]- $\sigma\eta$  rearrangement reaction. The same two-step pathway is observed when one carbonyl ligand of the cycloheptatriene complex is substituted by a phosphite or phosphine ligand, but reactions are faster. Previous studies with cycloheptatriene [2,4,5,18], tropone [3,19,20] and azepine [21]  $\eta^4$ -complexes of iron and ruthenium with a variety of dienophiles (such as TCNE, CMA and PTAD) show that the kinetically controlled cycloaddition step is highly periselective affording 3 + 2- $\sigma,\eta$ -adducts regardless of the dienophile, the seven-membered cyclic triene, or ligand carbonyl substitution. This suggests that the cycloaddition step is controlled by the nature of the metal, and Group 8 iron and ruthenium metal complexes selectively prefer the 3 + 2 cycloaddition route. Preliminary studies by Takats [22] show that the osmium analogs behave similarly. However, we now have evidence that this rule is not followed by  $\eta^4$ -cycloheptatriene complexes of Group 9 transition metals [23].

While we observe selectivity in cycloadditions, the order of the subsequent thermodynamically controlled sigmahaptotropic rearrangements is hard to predict. Thus, while the TCNE 3 + 2 adducts of cycloheptatriene and *N*-methoxycarbonylazepine iron complexes

rearrange to symmetrical 6 + 2 adducts via a 4,4- $\sigma\eta$  shift, the corresponding tropone complexes of TCNE and PTAD give mainly the 5 + 2 adducts, via a 3,3- $\sigma\eta$  shift. Finally, this study established that the 3 + 2 CMA iron complexes rearrange via a 2,2- $\sigma\eta$  shift to the 4 + 2 adducts. Interestingly, we notice that the analogous (cht)Ru(CO)<sub>3</sub> 3 + 2 complexes with either one of the above dienophiles remain stable [4] under the thermal conditions employed for the iron counterparts. This has been attributed to the increase in  $\sigma$ -bonding overlap of M–C bonds within the triads of Groups 7 and 9 [24].

#### 5. Experimental

IR spectra were measured with a Nicolet 60 SXB FT-IR spectrometer (KBr). Mass spectra were determined with a GC–MS Finnigan model 4021 spectrometer. <sup>1</sup>H- and <sup>13</sup>C-NMR spectra were recorded on a Bruker AM300 spectrometer with TMS as an internal standard. <sup>31</sup>P-NMR spectra were taken on a Bruker AC200 spectrometer, using 85% H<sub>3</sub>PO<sub>4</sub> as external standard. Solutions for NMR measurements were filtered over Celite shortly before use and purged with nitrogen. The sample temperatures were measured with a Urotherm 840/T digital thermometer, and are estimated to be correct within  $\pm 0.5^\circ\text{C}$ . All reactions were conducted under dry nitrogen.

##### 5.1. Preparation of starting materials

CMA was prepared by a modification of the procedure reported by Hall et al. [7], and purified (95–98% by NMR) by distillation under reduced pressure at 120°C (0.2 Torr). The parent iron complex (cht)Fe(CO)<sub>3</sub>, prepared according to Bochmeulen and Parkins [25], was distilled at 80°C (0.1 Torr) and kept (as a solid) in the freezer under nitrogen.

The phosphite complex (cht)Fe(CO)<sub>2</sub>P(OPh)<sub>3</sub> was prepared according to Pearson and Chen [9] and was purified (>95% by NMR) by repeated recrystallization from methanol. M.p. 102–103°C. <sup>1</sup>H-NMR (CDCl<sub>3</sub>)  $\delta$  7.34 (6H) and 7.20 (9H) (aromatic), 5.02 (1H, m), 4.67 (2H, m), 3.10 (1H, m), 2.80 (1H, m), 2.23, 2.05 (2H, AB q). <sup>31</sup>P-NMR (CDCl<sub>3</sub>)  $\delta$  165.2. IR (CDCl<sub>3</sub>) 2000, 1940, 1590 cm<sup>-1</sup>.

The phosphine complex (cht)Fe(CO)<sub>2</sub>PPh<sub>3</sub> prepared according to Johnson et al. [11] was purified by column chromatography (silica gel, ethyl acetate–hexane) and recrystallization (ether–pentane). M.p. 136–7°C (lit. [11] 137°C). <sup>1</sup>H-NMR (CDCl<sub>3</sub>)  $\delta$  7.34–7.35 (15H, aromatic), 5.81 (1H, ddd), 5.11 (1H, dt), 4.73 (2H, m), 2.65 (1H, m), 2.49 (1H, td), 2.36, 2.05 (2H, AB q). <sup>31</sup>P-NMR (CDCl<sub>3</sub>)  $\delta$  63.7. IR (KBr) 1973, 1920 cm<sup>-1</sup>.

5.2. Synthesis of the 4 + 2 adduct of CMA and (cht)Fe(CO)<sub>2</sub>P(OPh)<sub>3</sub> (**6**) (L = P(OPh)<sub>3</sub>)

Solutions of CMA (22.5 mg, 140 μmol) and (cht)Fe(CO)<sub>2</sub>P(OPh)<sub>3</sub> (60 mg, 120 μmol) in CH<sub>2</sub>Cl<sub>2</sub> were mixed together at room temperature for 1 h. Removal of the solvent and column chromatography (silica gel, CHCl<sub>3</sub>) afforded 41 mg (50% yield) of the phosphite adduct **6** as yellow crystals. M.p. 144–146°C (from CH<sub>2</sub>Cl<sub>2</sub>–hexane). Anal. Found: C, 59.12; H, 4.06. Calc. for C<sub>33</sub>H<sub>27</sub>FeO<sub>10</sub>P: C, 59.05; H, 4.12%. MS (DCI, methane): 671 (MH<sup>+</sup>, 98%), 639 (80), 615 (18), 577 (39), 515 (12), 459 (21), 421 (12), 389 (18), 365 (15), 356 (20), 311 (32), 249 (18), 245 (14), 217 (100). IR (KBr): 1985, 1942 (CO ligand), 1844, 1774 (anhydride CO), 1731 (ester CO), 1583, 1477 cm<sup>-1</sup>. For <sup>1</sup>H- and <sup>13</sup>C-NMR spectra see Tables 1 and 2, respectively.

## References

- [1] J. Weaver, P. Woodward, J. Chem. Soc. (A) (1971) 3521.
- [2] M. Green, S. Heathcock, D.C. Wood, J. Chem. Soc. Dalton Trans. (1973) 1564.
- [3] M. Green, S.M. Heathcock, T.W. Turney, D.M.P. Mingos, J. Chem. Soc. Dalton Trans. (1977) 204.
- [4] Z. Goldschmidt, E. Genizi, H.E. Gottlieb, D. Hezroni-Langermann, H. Berke, H.W. Bosch, J. Takats, J. Organomet. Chem. 420 (1991) 419.
- [5] Z. Goldschmidt, H.E. Gottlieb, E. Genizi, D. Cohen, I. Goldberg, J. Organomet. Chem. 301 (1986) 337.
- [6] Z. Goldschmidt, E. Genizi, H.E. Gottlieb, J. Organomet. Chem. 368 (1989) 351.
- [7] H.K. Hall Jr., P. Nogues, J.W. Rhoades, R.C. Sentman, M. Detar, J. Org. Chem. 47 (1982) 1451.
- [8] Z. Goldschmidt, S. Antebi, H.E. Gottlieb, D. Cohen, U. Shmueli, Z. Stein, J. Organomet. Chem. 282 (1985) 369.
- [9] A.J. Pearson, B. Chen, J. Org. Chem. 50 (1985) 2587.
- [10] F.M. Chaudhari, P.L. Pauson, J. Organomet. Chem. 5 (1966) 78.
- [11] B.F.G. Johnson, J. Lewis, M.V.J. Twigg, J. Chem. Soc. Dalton Trans. (1974) 2546.
- [12] Z. Goldschmidt, H.E. Gottlieb, J. Organomet. Chem. 329 (1987) 391.
- [13] J.A.S. Howell, A.D. Squibb, Z. Goldschmidt, H.E. Gottlieb, A. Almadhoun, I. Goldberg, Organometallics 9 (1990) 80.
- [14] J.A.S. Howell, A.G. Bell, D. Cunningham, P. McArdle, T.A. Albright, Z. Goldschmidt, H.E. Gottlieb, D. Hezroni-Langerman, Organometallics 12 (1993) 2541.
- [15] A.A. Frost, R.G. Pearson, Kinetic and Mechanism, 2nd edn, Wiley, New York, 1961.
- [16] J.F. Bunnett, in: E.S. Lewis (Ed.), Investigation of Rates and Mechanisms of Reactions, Part 1, 3rd ed., Wiley-Interscience, New York, 1964, p. 367.
- [17] H.K. Hall Jr., A.B. Padias, Acc. Chem. Res. 23 (1990) 3.
- [18] Z. Goldschmidt, E. Genizi, Synthesis (1985) 949.
- [19] Z. Goldschmidt, H.E. Gottlieb, D. Cohen, J. Organomet. Chem. 294 (1985) 219.
- [20] Z. Goldschmidt, H.E. Gottlieb, A. Almadhoun, J. Organomet. Chem. 326 (1987) 405.
- [21] S.K. Chopra, D. Cunningham, S. Kavanagh, P. McArdle, G. Moran, J. Chem. Soc. Dalton Trans. (1987) 2927.
- [22] J. Takats, personal communication.
- [23] E.g. with (cht)CoCp complex, to be published.
- [24] T. Ziegler, V. Tschinke, A. Becke, J. Am. Chem. Soc. 109 (1987) 1351.
- [25] H.A. Bochmeulen, A.W. Parkins, J. Chem. Soc. Dalton Trans. (1981) 262.